

Inelastic collisions of electrons with noble-gas ions

I. P. Zapesochnyi, A. I. Imre, and Ya. N. Semenyuk

Uzhgorod Division, Nuclear Physics Institute of the Ukrainian Academy of Sciences

(Submitted 25 April 1990)

Zh. Eksp. Teor. Fiz. 99, 721–734 (March 1991)

The excitation of lower levels of noble-gas ions and of dielectron recombination of the helium ion are investigated systematically and in detail, using the technique of intersecting modulated electron and ion beams and detecting the concomitant radiation in a wide spectral range (30–500 nm). The energy dependences of the effective excitation cross sections are investigated and their absolute values are determined for 32 spectral transitions. Distinct maxima are observed in the cross sections of the investigated processes, most of which are resonant. It is shown that the resonant maxima are due to formation and decay of autoionizing states in the corresponding electron and radiative channels.

1. INTRODUCTION

Collisions of low-energy electrons with noble-gas ions play an important role in various astrophysical objects, in laboratory plasma, and in the plasma of many technical installations. Of particular significance in the latter case are gas lasers (and other sources of light) in which the active medium is a plasma of noble gases or of other chemical elements with obligatory admixture of inert gases.

Investigation of inelastic processes in interactions of low-energy electrons with noble-gas atoms is therefore quite urgent. Reliable experimental data on collisions between electrons and such objects, primarily helium ions, are of substantial interest for atomic physics and for the development of a theory of electron collisions.

Our aim was a systematic and detailed investigation of the excitation of low-lying single-charge ions of noble gases by electron impact, and also of dielectron recombination of the helium atom, using detection of the concomitant radiation in the vacuum ultraviolet.

2. NOTES ON THE EXPERIMENTAL TECHNIQUE AND MEASUREMENT METHOD

Experiments with ions of noble and atmospheric gases are much more difficult than with metal ions.^{1,2} The complications are connected, on the one hand, with the method of obtaining a pure beam of singly charged gas ions, and on the other with ensuring an ultrahigh vacuum in the region of beam intersection. Moreover, radiation from noble-gas ions excited in various inelastic processes spans a rather large part of the spectrum—from the visible region to the vacuum ultraviolet (VUV), necessitating matching of the experimental setup to fundamentally different types of spectral instruments, including vacuum ones.

The employed experimental setup includes the following main units (see Fig. 1): another gas-discharge source (IS) of ions with the plasma pinched by a longitudinal magnetic field, a 180-degree mass spectrometer (MS) with a 0.5 m equilibrium trajectory radius of the ions (of energy 8–13 keV) a high-vacuum collision chamber differentially evacuated to a pressure $<10^{-7}$ Torr having an electron gun (EG) (electron energy 10–500 eV) and an electron collector (EC), a spectral monochromator (SM), stabilized power packs for the ion source and for the mass-spectrometer magnet, systems for modulating both beams (MSR), and for radiation detection (RD), and an ion collector (IC).

A pure beam of ions several keV in energy was produced by an ion-optical system and a 180-degree mass spectrometer with a nonuniform magnetic field. A charge-resolved beam of ions passed through differentially pumped vacuum sections into a collision chamber where it crossed an electron beam at 90°. The electrons came from a gun having three control electrodes placed in a longitudinal magnetic field.

The ion current density was maintained constant in the interaction region by stabilizing the discharge current, the ion-accelerating voltage, and the current in the magnetic mass spectrometer. The position of the ion beam on the input slit of the collision chamber was maintained by a servo-control circuit for the electromagnet current in the mass-spectrometer magnetic-field stabilization system. The vacuum chambers were differentially evacuated to $5 \cdot 10^{-8}$ Torr in the beam-crossing region.

The VUV radiation produced by the inelastic collisions was resolved by a vacuum monochromator developed in our laboratory, with normal (VM-70) or glancing (VM-140) incidence of the beams on a diffraction grating (1200 and 600 lines/mm, $R = 0.5$ and 1.0 m, respectively). For the visible region of the spectrum we used the commercial MDR-2 diffraction monochromator. The radiation was detected with secondary and photoelectron multipliers of type VEU-6 and FEU-106 (cooled), both operating in a single-electron pulse regime.

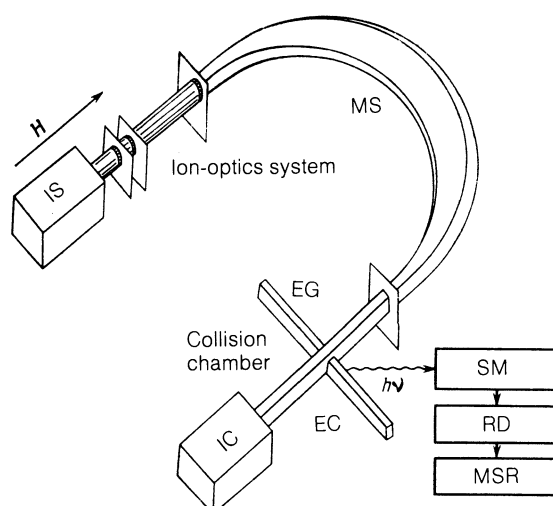


FIG. 1. Experimental setup.

Since the useful signal was substantially weaker than the background, the investigated radiation was recorded with both beams modulated by rectangular pulses shifted in phase by 1/4 period, and the amplified pulsed signal from the radiation detector was switched in synchronism with the modulation in two counting channels that accumulated the summary and background signals, respectively. Reversible accumulation of the signals during the measurement time yielded the sought useful signal. The recording system could separate the useful signal at a signal/background ratio up to 1/100.

All the experiments were performed under single-collision conditions. The ion and electron current densities were $(3-20) \cdot 10^{-4}$ and $(3-60) \cdot 10^{-3} \text{ A/cm}^2$. The respective ion and electron energy ranges were 8–13 keV and 10–500 eV, and the electron-inhomogeneity energy interval (at half the maximum of the distribution function) did not exceed 1–2

eV. The useful signal was 1.0–0.2 pulse/s at a signal/background ratio range 1/5–1/50.

We measured in control experiments the excitation functions of the spectral lines of the principal series of the helium atom and ion in electron-ion collisions.³ The electron energy scale was calibrated against the excitation thresholds of these spectral lines, accurate to ± 0.25 eV.

3. RESULTS AND THEIR DISCUSSION

1. In a series of prolonged experiments, in the visible and particularly in the VUV regions of the spectrum, we measured the excitation functions (EF) and determined the effective excitations cross sections (EEC) of optically resolved (resonance lines) and optically forbidden transitions of noble gases, as well as of spectral transitions connected with electron excitation from the subvalent ns^2 subshell of

TABLE I. Effective cross sections for excitation of spectral transitions of noble-gas ions by electron impact.

Ion	Transition	λ , nm	E_{max} , eV	$\sigma_{max} \cdot 10^{-19} \text{ cm}^2$
He ⁺	$(1s)^2S - (2p)^2P^0$	30,4	44; 47; 49; 60 *	0,8
	$(3d)^2D - (4s)^2F^0$	468,6	54; 60 *	0,12
Ne ⁺	$(2s^2p^5)^2P^0 - (2s^2p^43s)^2,4P + (2s^2p^6)^2S$	44,5–46,2	28; 37 *; 45; 65	43,0
Ar ⁺	$(3s^23p^5)^2P^0 - 3s^23p^43d' 2P, 2D$	57,2–58,0	22; 24 *; 28	10,0
	$(3s^23p^5)^2P^0 - (3s^23p^44s', 3d)^2D, 4P$	66,1–68,0	18,5 *; 20; 22,5; 25	12,0
	$(3s^23p^5)^2P^0 - (3s^23p^44s)^2P$	71,8–72,3	18 *; 21	14,0
	$(3s^23p^5)^2P^0 - (3s3p^6)^2S$	91,9; 93,2	14 *; 15; 17; 22	20,0
	$(3s^23p^44s)^2P_{1/2} - (3s^23p^44p)^2D_{3/2}^0$	496,5	22; 28 *	0,44
	$(3s^23p^44s)^2P_{3/2} - (3s^23p^44p)^2D_{5/2}^0$	488,0	22; 29 *	1,3
	$(3s^23p^44s)^4P_{1/2} - (3s^23p^44p)^4P_{1/2}^0$	480,6	21; 26 *	0,28
	$(3s^23p^44s)^2P_{1/2} - (3s^23p^44p)^2P_{3/2}^0$	476,5	22; 30 *	0,3
	$(3s^23p^44s)^2P_{3/2} - (3s^23p^44p)^2P_{1/2}^0$	465,8	22; 29 *	0,35
	$(3s^23p^44s')^2D_{3/2} - (3s^23p^44p')^2F_{1/2}^0$	461,0	22,5; 34 *	0,5
	$(3s^23p^44s)^2P_{1/2} - (3s^23p^44p)^2S_{1/2}^0$	457,9	22; 35 *	0,2
	$(3s^23p^44s)^2P_{3/2} - (3s^23p^44p)^2P_{3/2}^0$	454,5	22; 29 *	0,15
	$(3s^23p^44s)^4P_{3/2} - (3s^23p^44p)^4D_{3/2}^0$	434,8	21; 30 *	0,25
	$(3s^23p^44s')^2D_{3/2} - (3s^23p^44p)^2P_{1/2}^0$	413,1	23; 31 *	0,1
Kr ⁺	$(4s^24p^5)^2P^0 - (4s^24p^44d')^2F, 2D$	66,3–66,9	19,5; 21,5	10,0
	$(4s^24p^5)^2P^0 - (4s^24p^44d, 5s)^2D$	78,2–78,4	16,5; 19,5 *; 22	13,0
	$(4s^24p^5)^2P^0 - (4s^24p^44d, 5s)^2,4P, 4D$	85,9–86,8	15,5 *; 17,5; 20	15,0
	$(4s^24p^5)^2P^0 - (4s^24p^45s)^4P + (4s^24p^6)^2S$	91,1–91,7	14; 16; 22 *	10,0
	$(4s^24p^45s)^4P_{3/2} - (4s^24p^45p)^4D_{3/2}^0$	476,6	18; 24 *	0,4
	$(4s^24p^45s)^4P_{3/2} - (4s^24p^45p)^4P_{3/2}^0$	473,9	18; 23 *	0,36
	$(4s^24p^45s)^4P_{3/2} - (4s^24p^45p)^4P_{1/2}^0$	465,9	17; 24 *	0,25
	$(4s^24p^45s')^2D_{3/2} - (4s^24p^45p')^2F_{1/2}^0$	463,4	20; 27 *	0,2
	$(4s^24p^45s')^2D_{3/2} - (4s^24p^45p')^2I_{1/2}^0$	457,7	20; 27 *	0,5
	$(4s^24p^45s')^2D_{3/2} - (4s^24p^45p')^2P_{3/2}^0$	447,5	20; 30 *	0,1
	$(4s^24p^45s)^4P_{3/2} - (4s^24p^45p)^4D_{3/2}^0$	435,5	19; 29 *	0,15
	$(4s^24p^45s)^4P_{3/2} - (4s^24p^45p)^4D_{5/2}^0$	429,3	19; 29 *	0,1
	$(4s^24p^45s')^2D_{3/2} - (4s^24p^45p')^2D_{3/2}^0$	408,8	22; 30 *	0,12
Kr ²⁺	$(4s^24p^35s)^3S_1^0 - (4s^24p^35p)^3P_2$	350,7	28; 37 *	1,8
	$(4s^24p^35s)^5S_2^0 - (4s^24p^35p)^5P_1$	335,2	24; 45 *	0,7

Notation: E_{max} —energy corresponding to maximum; σ_{max} —maximum cross section.

* The energy values corresponding to the maximum cross section in the next column.

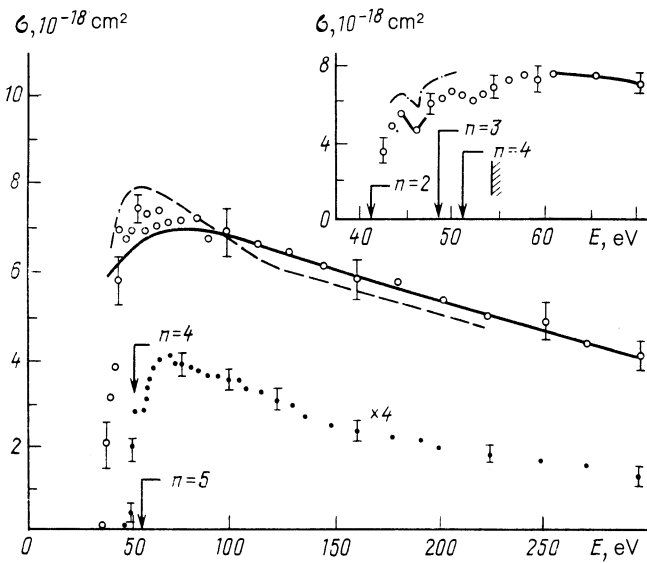


FIG. 2. Energy dependences of the cross sections for He^+ ion level excitation: ○—experiment for $2p$ level ($\Delta E_{1/2} = 2 \text{ eV}$; solid line—calculation in the KBII approximation⁴; dashed—calculation in the tight-binding approximation;⁹ ●—experiment for 4^2L levels ($\Delta E_{1/2} = 1 \text{ eV}$). Inset: ○—initial section of energy dependence of the $2p$ -level excitation cross section ($\Delta E_{1/2} = 1 \text{ eV}$); dash-dot—calculated by the diagonalization method and averaged with allowance for the instrumental function with $\Delta E_{1/2} = 1 \text{ eV}$.¹⁰

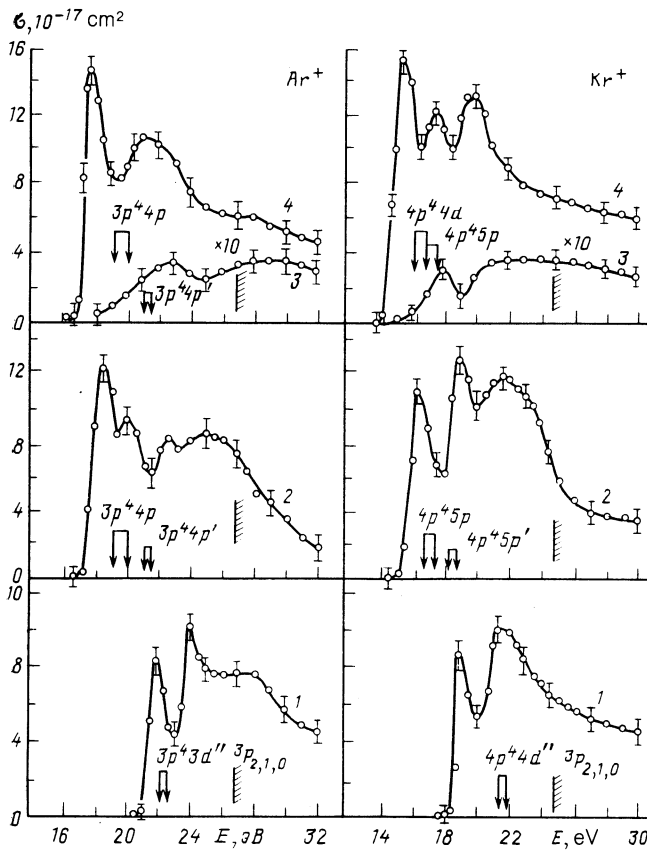


FIG. 3. Energy dependences of the cross sections for excitation of spectral transitions: 1— $\lambda = 57.2\text{--}58.0 \text{ nm}$ [transition $(3p^4 3d') ^2P^2 D \rightarrow (3p^5)^2 P^0$, Ar^+ ion] and $\lambda = 66.3\text{--}66.9 \text{ nm}$ (transition $(4p^4 4d') ^2D, ^2F \rightarrow (4p^5)^2 P^0$, Kr^+ ion); 2— $\lambda = 66.1\text{--}67.9 \text{ nm}$ (transition $(3p^4 3d, 4s') ^4P, ^2D \rightarrow (3p^5)^2 P$, Ar^+ ion) and $\lambda = 78.2\text{--}78.4 \text{ nm}$ (transition $(4p^4 4d, 5s)^2 P \rightarrow (4p^5)^2 P^0$, Kr^+ ion); 3— $\lambda = 465.8 \text{ nm}$ (transition $(4p)^2 P_{1/2} \rightarrow (4s)^2 P_{3/2}$, Ar^+ ion) and $\lambda = 473.9 \text{ nm}$ (transition $(5p)^4 P_{5/2} \rightarrow (5s)^4 P_{5/2}$, Kr^+ ion); 4— $\lambda = 71.8\text{--}72.3 \text{ nm}$, (transition $3p^4 4s)^2 P \rightarrow (3p^5)^2 P^0$, Ar^+ ion) and $\lambda = 85.9\text{--}86.8 \text{ nm}$ (transition $4p^4 4d, 5s)^2 P \rightarrow (4p^5)^2 P^0$, Kr^+ ion).

Ne^+ , Ar^+ , and Kr^+ ions. The results are listed in Table I and are shown in Figs. 2–4 as plots of the effective excitation cross sections of the spectral lines vs the bombarding-electron energy E . In addition, we investigated for the helium ion, in the energy interval 32–41 eV and in the spectrum range 30–32 nm, the excitation of the radiation produced by dielectron recombination (Fig. 5).

The signal at each experimental point was the accumulated result of 7–10 measurements with exposures 1000 s and longer. The reproducibility of the results was verified in numerous measurements under various experimental conditions. The rms relative EF-measurement error did not exceed $\pm (10\text{--}15)\%$.

The absolute value of the cross section σ_{res} for the excitation of a helium-ion resonance line was determined by normalizing the experimental data at $10E_{\text{thr}}$ to the calculated excitation cross sections of the $2p$ level of He^+ , using the second Coulomb–Born approximation⁴ (see Fig. 2).¹¹ The

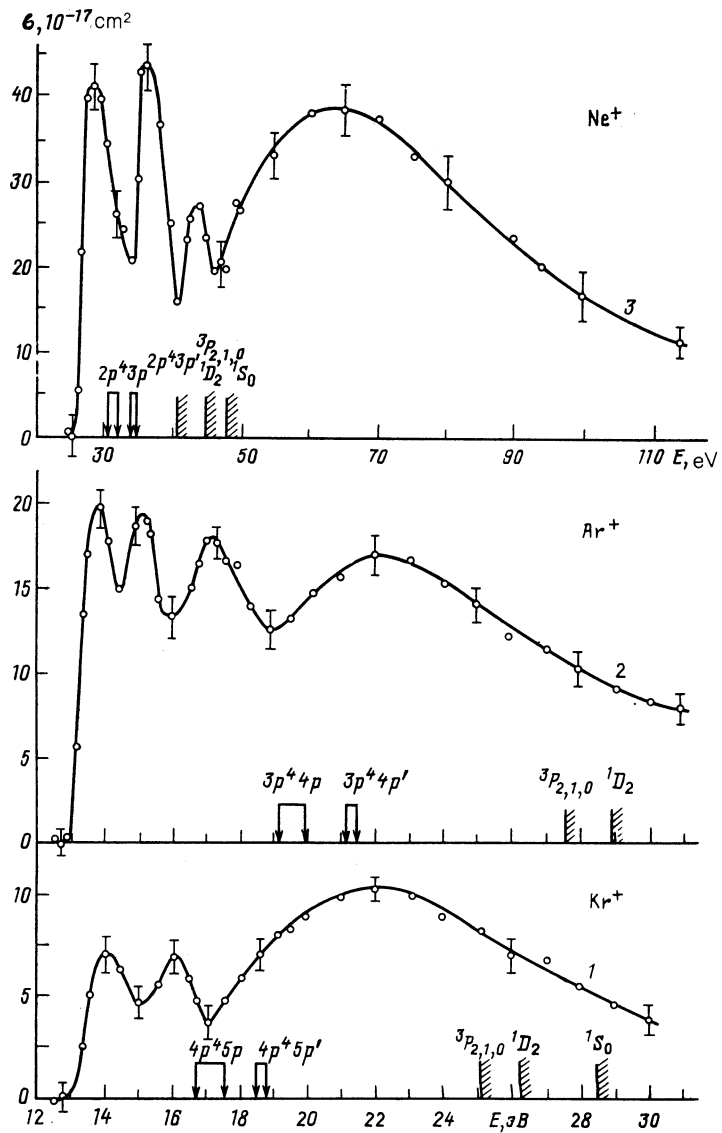


FIG. 4. Energy dependences of the cross sections for the excitation of spectral transitions: 1— $\lambda = 91.1\text{--}91.7 \text{ nm}$ (transition $[(4s4p6)^2S + (4p4s5)^2P] \rightarrow (4s^24p^5)^2P^0$, Kr^+ ion); 2— $\lambda = 91.9\text{--}93.2 \text{ nm}$ (transition $(3s3p^5)^2S \rightarrow (3s^23p^5)^2P^0$, Ar^+ ion); 3— $\lambda = 44.5\text{--}46.2 \text{ nm}$ (transition $[(2s2p^6)^2S + (2s^22p^43s)^2P] \rightarrow (2s^22p^5)^2P^0$, Ne^+ ion).

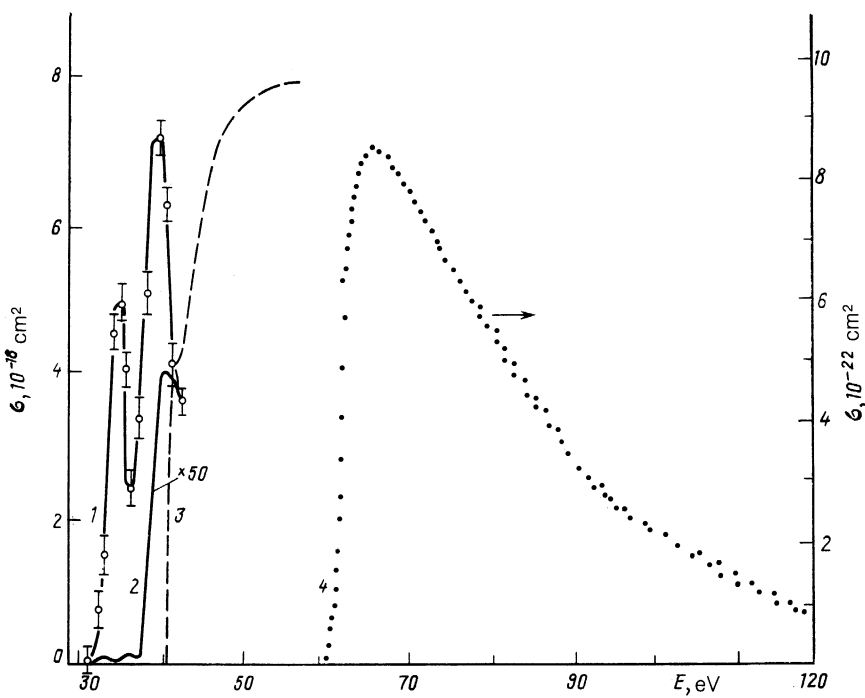


FIG. 5. Energy dependences of cross sections for radiation excitation at wavelengths $\lambda = 30\text{--}32 \text{ nm}$, He atom: 1—experiment, electron-ion collisions; 2—calculation by the diagonalization method, averaged with allowance for instrumental function with $\Delta E_{1/2} = 1 \text{ eV}$ (Ref. 22); 3—initial section of the energy dependence of the cross section for excitation of $2p$ level of He^+ ion; 4—experiment, electron-atom collisions.

absolute values of the excitation cross sections σ_1 of other spectral lines of noble-gas ions were obtained from the known cross sections for the same transitions excited by electron-atom collisions,^{6,7} using the expression

$$\sigma_\lambda = \frac{C N'_0 N'_e v'}{C' N'_i N'_e v} \sigma'_\lambda, \quad (1)$$

where (the primed quantities pertain to electron-atom collisions) C is the measured useful signal; N'_0, N'_i , and N'_e are, respectively, the densities of the atoms, ions and electrons; v is the electron velocity. The rms error of the absolute values of the excitation cross section did not exceed $\pm 30\%$ in this case.

We consider now in greater detail the singularities of the energy dependences of the effective excitation cross sections of the investigated spectral transitions and their origin.

2. We were able, for the first time ever, to investigate in detail excitation of a resonance line in the VUV region of the spectrum ($\lambda = 30.4 \text{ nm}$) by electrons of higher energy homogeneity, and spectral transitions between levels with principal quantum numbers $n = 4$ and 3 in the visible region ($\lambda = 468.6 \text{ nm}$). As seen from Fig. 2, the energy dependences of the excitation cross sections of these lines are in general close. They show, just as the analogous curves for alkali-metal ions,¹ a smooth decrease (following a broad maximum) of the excitation cross section, given by $\sigma \propto E^{-1} \ln E$. Substantial differences are observed at near-threshold energies (see inset of Fig. 2), where the EF of the resonance line exhibits a structure consisting of three maxima (see the table),² whereas the EF line with $\lambda = 468.6 \text{ nm}$ has only a kink. Furthermore, the first most clearly pronounced maximum on the resonance-line EF is close to the excitation threshold in the energy region where cascade transitions cannot occur at all.

One of the possible explanations of the nature of the observed structure may be additional population of a resonance $2p$ level of He^+ (on top of the direct process) as a result of electron transitions to this level from atomic autoionizing states formed as the ions capture bombarding

electrons. These atomic states, as is well known, are arranged in series that converge to the excited ion levels with given quantum number n . Nonradiative decay of such states (with emission of an electron) takes place predominantly to excited levels of the ion.

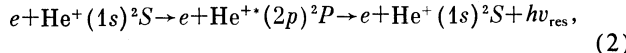
We turn now to the first maximum of the structure on the helium-ion EF resonance line ($\lambda = 30.4 \text{ nm}$). Its position correlates in energy with the positions of the autoionizing He-atom states that converge to an He^+ level with $n = 3$. The main channel of their decay, as shown in Ref. 11, is electron decay to lower helium-ion excited $n = 2$ levels, while the decay probability to the ground state of the ion is less than 1% of the total autoionization probability. In view of the foregoing it can be assumed that the first maximum on the EF resonance line is due to contribution to the $\text{He}^+ 2p$ level from electron decay of autoionizing states converging to $n = 3$ He^+ levels. Owing to the beam-electron energy inhomogeneity, which exceeds substantially the autoionizing-state widths, our experiments yielded only the average contribution of a whole group of autoionizing states.

As to the second maximum on the resonance line EF, it is also the result of electron capture by a helium ion with formation of lower autoionizing states whose subsequent decay can lead directly or via cascade transition to additional population of the $\text{He}^+ 2p$ level. For lack of published data on the decay channels of such autoionizing states, however, a more definite interpretation is impossible.

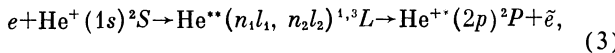
Our assumptions are well confirmed by recent theoretical calculations,¹⁰ where a diagonalization method (one of the variants of the tight-binding method) was used to calculate the excitation cross sections of a He^+ -ion resonant $2p$ level with account taken of 30 autoionizing states converging to He^+ levels with $n = 3$. The dash-dot line on the inset of Fig. 2 shows the theoretical dependence of the cross section for excitation of this level by electron impact, obtained in Ref. 10 by averaging of the electron inhomogeneity in this experiment. Good agreement is seen with respect to both the character of the structure and the absolute value of the effec-

tive excitation cross section.

It can thus be asserted that the population of the helium-ion $2p$ level (and correspondingly the emission of resonant radiation) occurs not only via the direct process



but also via formation of intermediate helium-atom autoionizing states (resonance process)



where n_1 and $n_2 \geq 3$ and \tilde{e} is the emitted electron. The contribution of the resonance process to the population of the $2p$ level of the helium ion is appreciable, 20% of the direct process.

As to excitation of an He^+ spectral line with $\lambda = 468.6$ nm, the contribution of the resonance processes to the population of the upper levels of this line is substantially weaker for this case. This agrees with theoretical papers^{10,11} where it is shown that the probability of formation of autoionizing states that converge to lower He^+ ion levels decreases significantly with increase of n .

3. For other noble-gas ions containing an external np^5 subshell, investigations were made of the excitation of resonance transitions from lower $(n+1)s$ and nd configurations that converge to $^3P_{2,1,0}$ and 1D_2 ionization limits, respectively, as well as of the excitation of the so-called laser transitions of Ar^+ , Kr^+ , and Kr^{2+} ions via radiative transitions between $(n+1)p$ - and $(n+1)s$ -levels (see Fig. 6). Also investigated were radiative transitions resulting from formation of internal vacancies $(nsnp^6)^2S_{1/2}$ in electron-ion collisions. The filling of such a vacancy by an electron from the np^6 subshell is accompanied by emission of an ultrasoft x-ray (USX) doublet.

The resonance and USX transitions of Ne^+ , Ar^+ , and Kr^+ ions lie in the vacuum ultraviolet region of the spectrum ($\lambda = 44-46$ nm). Owing to the large number of spec-

tral lines in a relatively narrow wavelength interval ($\lambda \sim 50$ nm), difficulties arise when it comes to identifying noble-gas ion spectra and become ever more complicated with increase of the atomic number of the ion. Separation of the spectral transition calls for a spectral resolution ~ 0.1 nm, difficult to attain under conditions of intersecting ion and electron beams, owing to the weakness of the detected useful signal. The latter can be compensated for only by one method—the use of relatively wide slits (~ 1.0 mm) in the VUV monochromators. It is possible, however, to investigate with acceptable accuracy the excitation of line groups of a single definite configuration. As to laser transitions of argon and krypton ions, they lie in the visible region of the spectrum and their excitation was investigated separately for each line.

Note that, as shown in Ref. 7, EF of a group of lines and of an individual spectral line of one ion configuration are similar. It can therefore be assumed that our measurement results reflect adequately the main features of the excitation of lower levels of noble gas ions, and that the accompanying information loss is not significant.

It follows from the results that the largest effective excitation cross sections (EEC) for argon and krypton ions are those of transitions with $nsnp^6$ and $ns^2np^4(n+1)s$ configurations. It should be noted that we investigated the excitation of a subvalent ns^2 subshells in pure form only for argon ions, and that transitions from $ns^2np^4(n+1)s$ configuration levels are superimposed on the radiation $nsnp^6$ levels of Ne^+ and Kr^+ .

We consider now the structures of the excitation-function plots for the investigated transitions. As seen from Figs. 3 and 4, the first maxima of all the curves are close to the threshold of the process, where there are no cascade transitions (for USX doublets this holds also for the second EF maximum of Kr^+ and for the second and third maxima of Ar^+ , see curves 1 and 2 of Fig. 4). We can therefore assume that these (first) maxima, just as in the case of the helium ion, are due to autoionization of atomic superexcited states

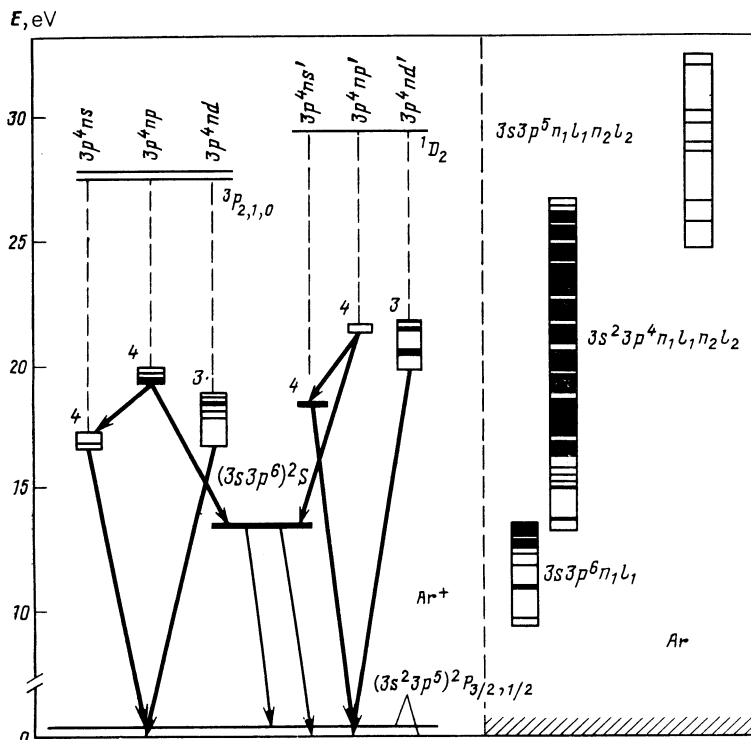
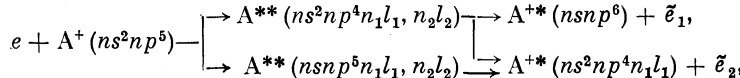


FIG. 6

produced when the ions capture the impinging electrons. This is attested to also by such facts as the energy positions and widths of the first maxima, and the presence of many autoionizing states just in these energy regions (see Fig. 6). Further, an investigation of the same transitions of noble-gas ions excited by electron-atom collisions also points to a noticeable role of the decay of autoionizing states.

Starting from the above considerations, we can state that beside the main process of direct excitation of the investigated states of type $A^{+*}(nsnp^6)$ and $A^{+*}(ns^2np^4n_1l_1)$, via the reactions



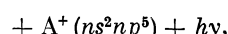
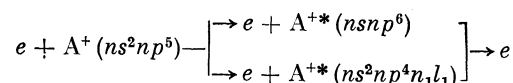
where \tilde{e}_1 and \tilde{e}_2 are electrons emitted upon restructuring of the outer shell of the atom. Convolution of these resonance with the instrumental function is observed here in experiment.

The published data (which, incidentally, are quite scanty) confirm to a certain degree the formation of both indicated types of autoionizing state. Some of them for neon, argon, and krypton were observed in investigations of photoabsorption¹² and of ion-atom collisions.¹³⁻¹⁶

It follows from the results that for noble-gas ions (except for helium) resonance excitation near the threshold of the process predominate over direct excitation. In excitation of resonance transitions, the produced autoionizing states decay via the Köster-Kronig effect, whereas the excitation of the subvalent ns^2 subshells of neon, argon and krypton ions the decay is via three-electron transitions with filling of the produced two np^4 -subshell vacancies, see Eq. (5).

As to the origin of the remaining maxima on the EF of resonance transitions, most of them are in a certain correspondence with the energies of the higher ion levels. One can therefore not exclude the possibility of cascade transitions from these levels. The most probable is a transition from $ns^2np^4(n+1)p$ configuration levels. These, however, are optically forbidden relative to the ground state and consequently, as shown in Ref. 17, their effective excitation is more than an order of magnitude smaller compared with the resonance levels (see curves 3 of Fig. 3). We add here that we have investigated the energy dependences in the visible region of the spectrum and determined the EEC for 21 laser transitions between the levels of the $3s^23p^4(4p, 4p')$ and $3s^23p^4(4s, 4s')$ configurations of Ar^+ and $4s^24p^4(5p, 5p')$ and $4s^24p^4(5s, 5s')$ configurations of Kr^+ , and also between the levels $4s^24p^35p$ and $4s^24p^35s$ of the Kr^{2+} configurations (see the table). The corresponding EF are similar in form and are characterized by two maxima. Here, too, the most probable near the excitation threshold is the contribution of the autoionizing states that decay directly to the upper levels of the investigated lines, or via a cascade transition.

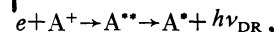
4. The role of electron capture is particularly impressive in one of the types of electron-ion recombination, called dielectron recombination. The neutral-atom autoionizing states formed in this process via electron capture decay in this case in a radiative channel with emission of a photon corresponding to a transition of a superexcited atom to an ordinary discrete level (located above the ionization threshold) of a neutral atom:



(4)

there is an additional fraction due to capture of the impinging electrons and to formation of superexcited neutral atoms, followed by the decay of autoionizing states:

(5,5')



(6)

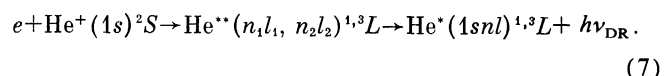
where $h\nu_{DR}$ is the radiation accompanying the dielectron recombination.

Electron capture in dielectron recombination is resonant: it is possible within the confines of an autoionizing level in the vicinity of a fixed energy of the impinging electrons. In most cases, radiative decay of autoionizing states in dielectron recombination is to high-lying levels of the atom ($n \gg 1$).

In our present investigation of He^+ ion excitation we were able, for the first time ever, to observe radiation produced in the 30–32 nm region at impinging-electron energies lower than the excitation threshold of the lowest resonance level of the helium atom (see curve 1 of Fig. 5).¹⁸ We note here that spectral lines in the 30–32 nm region were observed also in the spectrum produced by passage of a fast helium-ion beam ($E \sim 300$ keV) through a metal foil,¹⁹ the most intense being the line with $\lambda = 32$ nm, which is listed in the spectral-line table²⁰ as decay of an autoionizing state of the He atom [$(2p^2)^3P - (1s2p)^3P$ transition]. We have also investigated the EF of the $\lambda = 32$ nm spectral line in electron collisions with neutral helium atoms. The corresponding energy dependence of the EEC is represented by curve 4 of Fig. 5. Evidently its cross section is small ($\sim 10^{-21} \text{ cm}^2$ at the maximum), it is excited in a rather wide electron-beam energy region (60–120 eV), and the decrease of the cross section past the maximum near the threshold is well described by the relation $\sigma \propto E^{-3}$ typical of processes with change of spin.

At the same time, for electron-ion collisions, emission in the 30–32 nm region (see curve 1, Fig. 5) is observed in a narrow energy interval ($\Delta E < 10$ eV) in the form of two distinct maxima. It should be emphasized that this impinging-electron energy region contains a large number of autoionizing He states, investigated in detail in Ref. 21, which converge to the excited levels of He^+ with $n = 2$.

It can be unequivocally concluded from the considered aggregate of data that the considered radiation (produced below the excitation threshold of the $He^+ 2p$ level) occurs in dielectron recombination of helium atoms in accordance with the reaction



(7)

The cross section was determined by comparing the dielectron-recombination radiation intensity with the 30.4-nm

He^+ resonance line, close to it in wavelength and excited by electron-ion collisions (see curve 3 of Fig. 5).

We examine now in greater detail the character of the dielectron-recombination radiation. Evidently (Fig. 5) the energy widths of the maxima of its EF are comparable with the energy inhomogeneity of the electron beam. It can therefore be assumed that the structure is governed by capture of an impinging electron by a helium atom and subsequent radiative stabilization of an autoionizing He state that converges to the excited He^+ levels with $n = 2$. The cause of the first maximum is here the contribution of low-lying autoionizing states, particularly $(2p^2)^3P$ states of He , while the second maximum is the result of the summary contribution from high autoionizing states.

Figure 5 shows a comparison of the experimental results with a theoretical calculation²² (curve 2) of dielectron recombination of He^+ , with account taken of 50 He-atom upper states with $2snl$ and $2pnl'$ configurations (n and $n' \leq 5$) that decay to levels with $1snl$ configurations (where $n \leq 6$). The theoretical curve is a convolution of the calculation results with an instrumental function having a half-width $\Delta E_{1/2} = 1 \text{ eV}$.

As to the absolute value of the dielectron-recombination cross section, its experimental value exceeds the calculated by more than one order. Possible causes of the disparity are, on the one hand, the insufficient number of the autoionizing states taken into account in Ref. 22, and on the other to the influence of the longitudinal magnetic field ($H \sim 0.01 \text{ T}$) in which the electron beam is focused. An appreciable electric field is produced in the latter case in the rest frame of the ion and increases to a certain degree the cross section for dielectron recombination. It follows thus from Ref. 23 that an electric field of intensity 5–50 V/cm can alter the dielectron-recombination cross section at the maximum by more than an order of magnitude. Calculations of Ref. 23 for the Mg^+ ion with allowance for the influence of the magnetic field agree satisfactorily with experiment. Obviously, further experimental and theoretical investigations are needed for a better understanding of the features of dielectron recombination.

4. CONCLUSION

The lower levels of noble-gas ions are populated by electron impact not only when they are excited from the ground state. A significant role is played here by capture of an impinging electron by an ion to form autoionizing states of a neutral atom and their subsequent decay to excited levels of a resonance ion. Additional population of lower levels

of ions excited by an electron beam takes place predominantly in the electron channel. Resonance transitions decay then mainly via the Köster-Kronig effect, while for excitation of the subvalent ns^2 subshell the decay is via three-electron transitions with filling of the produced divacancy in the np^4 subshell. Radiative stabilization of the system on the excited levels of the neutral atom, with photon emission, takes place for dielectron recombination.

Further progress in the understanding of ion-excitation mechanisms depends substantially on the feasibility of observing isolated resonances when the energy homogeneity of electron beams is substantially improved.

¹⁾ Note that the contribution of cascade transitions (from higher levels) to the population of the resonance $2p$ level of He^+ , as follows from theoretical calculations,⁵ is small (8–10%). The experimental curve of Fig. 2 is therefore in practice a plot of the excitation of just the $2p$ level of He^+ .

²⁾ This was reported in a brief communication.⁸

- ¹I. P. Zapesochnyi, V. A. Kel'man, A. I. Imre *et al.*, Zh. Eksp. Teor. Fiz. **69**, 1948 (1975) [Sov. Phys. JETP **42**, 989 (1975)].
- ²W. T. Rogers, G. H. Dunn, J. O. Olsen *et al.*, Phys. Rev. A **25**, 681 (1982).
- ³Ya. N. Semenyuk, A. I. Imre, A. I. Dashchenko, and I. P. Zapesochnyi, Opt. Spektrosk. **55**, 430 (1983).
- ⁴A. Burgess, D. G. Hummer, and J. A. Tully, Phil. Trans. Roy. Soc. (London) A **266**, No. 1176, 225 (1970).
- ⁵J. A. Fully, Canad. J. Phys. **51**, 2047 (1973).
- ⁶I. P. Zapesochnyi and I. V. Pel'tsan, Ukr. Fiz. Zh. **10**, 1197 (1965).
- ⁷V. -F. Z. Papp, Deposited paper, VINITI No. 4501-76 (1976), p. 35.
- ⁸Ya. N. Semenyuk, Ukr. Fiz. Zh. **29**, 1252 (1984).
- ⁹P. G. Burke, D. D. McVicar, and K. Smith, Proc. Roy. Soc. London **83**, 397 (1964).
- ¹⁰M. I. Gaisak, V. I. Lend'el, V. T. Navrotskii, and E. P. Sabad, Ukr. Fiz. Zh. **27**, 1617 (1982).
- ¹¹V. S. Senashchenko and A. Waque, J. Phys. B **12**, L269 (1979).
- ¹²R. P. Madden, D. L. Ederer, and K. Codling, Phys. Rev. **177**, 136 (1969).
- ¹³G. N. Ogurtsov, I. P. Flaks, and S. V. Avakyan, Zh. Eksp. Teor. Fiz. **57**, 27 (1969) [Sov. Phys. JETP **30**, 16 (1969)].
- ¹⁴K. Jorgensen, N. Andersen, and O. J. Olsen, J. Phys. B **11**, 2951 (1978).
- ¹⁵J. O. Olsen, T. Andersen, and M. Barat, Phys. Rev. A **19**, 1457 (1979).
- ¹⁶K. Codling and R. P. Madden, Phys. Rev. Lett. **12**, 106 (1964).
- ¹⁷I. P. Zapesochnyi, A. I. Imre, A. I. Daschenko *et al.*, Zh. Eksp. Teor. Fiz. **63**, 2000 (1972) [Sov. Phys. JETP **36**, 1056 (1972)].
- ¹⁸I. P. Zapesochnyi, Ya. N. Semenyuk, A. I. Dashchenko *et al.*, Pis'ma Zh. Eksp. Teor. Fiz. **39**, 120 (1984) [JETP Lett. **39**, 141 (1984)].
- ¹⁹H. G. Berry, J. Desesquelles, and M. Dufau, Phys. Rev. A **6**, 600 (1972).
- ²⁰A. R. Striganov and G. A. Odintsova, *Tables of Spectral Lines of Atoms and Ions* [in Russian], Energoizdat (1982), p. 312.
- ²¹W. Shearer-Izumi, Data and Nucl. Data Tables **20**, 531 (1977).
- ²²O. I. Zatsarinny, V. I. Lengyel, and E. P. Sabad, Abstr. of Contributed Papers, XIII Conf. Phys. Electron and Atom Collisions, Berlin, 1983, p. 749.
- ²³K. La Gattula and J. Hahn, Phys. Rev. Lett. **51**, 558 (1983).

Translated by J. G. Adashko